

First passage time for subdiffusion: Nonextensive entropy approach versus fractional model

Tadeusz Kosztolowicz*

*Institute of Physics, Jan Kochanowski University,
ul. Świętokrzyska 15, 25-406 Kielce, Poland.*

Katarzyna D. Lewandowska†

*Department of Radiological Informatics and Statistics,
Medical University of Gdańsk,
ul. Tuwima 15, 80-210 Gdańsk, Poland.*

(Dated: February 6, 2019)

We study the similarities and differences between different models concerning subdiffusion. More particularly, we calculate first passage time (FPT) distributions for subdiffusion, derived from Green's functions of nonlinear equations obtained from Sharma–Mittal's, Tsallis's and Gauss's nonextensive entropies. Then we compare these with FPT distributions calculated from a fractional model using a subdiffusion equation with a fractional time derivative. All of Green's functions give us exactly the same standard relation $\langle(\Delta x)^2\rangle = D_\alpha t^\alpha$ which defines subdiffusion ($0 < \alpha < 1$), but generally FPT's are not the equivalent of to one another. We will show here that the FPT distribution for the fractional model is equal to the Sharma–Mittal model only if in the latter r depends on α , and satisfies the specific equation derived in this paper, whereas the other two models mentioned above give different FPTs with the fractional model. Green's functions obtained from the Sharma–Mittal and fractional models – for r obtained from this particular equation – are very similar to each other. We will also discuss the interpretation of subdiffusion models based on nonextensive entropies and the possibilities of experimental measurement of the subdiffusion models parameters.

PACS numbers: 02.50.Ey, 05.40.-a, 66.10.C-, 05.70.Ln

I. INTRODUCTION

Over about the last 20 years the anomalous diffusion process has been observed in many physical systems. Simultaneously, various theoretical models of this process have been put forward (see [1–3] and the references cited therein). The definition of the anomalous diffusion equation is rather vague and can be expressed by the following formula: *Any equation whose fundamental solution (Green's function) $G(x, t; x_0)$ provides the relation*

$$\langle(\Delta x)^2\rangle = D_\alpha t^\alpha, \quad (1)$$

with $\alpha > 0$, $\alpha \neq 1$ and

$$\langle(\Delta x)^2\rangle = \int_{-\infty}^{\infty} x^2 G(x, t; x_0) dx,$$

can be treated as an equation describing the anomalous diffusion process. Throughout this paper we have assumed that we are dealing with one-dimensional homogeneous systems without any external fields and convective flows; here D_α is the anomalous diffusion coefficient measured in the units m^2/s^α and α is the anomalous diffusion parameter, $0 < \alpha < 1$ for subdiffusion, $\alpha > 1$ for

superdiffusion; and when $\alpha = 1$ we are dealing with normal diffusion. Thus, anomalous diffusion is controlled by two parameters: D_α and α . We would like to add that the anomalous diffusion coefficient is sometimes defined differently, for example the subdiffusive coefficient \tilde{D}_α is often defined as [2, 3] $\tilde{D}_\alpha = \Gamma(1 + \alpha)D_\alpha/2$. The most used anomalous diffusion models are the Continuous Time Random Walk (CTRW) model and the models derived from nonextensive entropies. Throughout this paper we will refer to the model based on CTRW as a fractional model. CTRW provides the linear anomalous diffusion equation with the fractional-order derivatives [2–4], while the models based on the nonextensive Sharma–Mittal, Tsallis and Gauss entropies give nonlinear differential (or integral–differential) equations with derivatives of a natural order [5–14]. We should remark here that such equations were also derived from the generalized Langevine equation [15–19] and from the master equation [20]. The simplest stochastic interpretation of the anomalous diffusion seems to be found within CTRW models, where the random walker waits an anomalously long time to make its next step, for example in the transport process of sugars in gel (for subdiffusion) or where the step length can be anomalously long with a relatively high probability, for example a random walk in a turbulent medium (for superdiffusion). For the nonextensive entropy model a physical meaning to the anomalous diffusion equation is manifested mainly in its stationary version, namely, the stationary solution of the equation maximizes the nonextensive entropy. Although Green's func-

* <http://ujk.edu.pl/stroony/Tadeusz.Kosztolowicz/>;
tadeusz.kosztolowicz@ujk.kielce.pl

† kale@gumed.edu.pl

tions derived from the equation mentioned above provide Eq. (1), other important characteristics, such as a first passage time distribution, are different.

First passage time (FPT), which is one of the most important characteristics in normal and anomalous diffusions [21, 22], was studied for anomalous diffusion mainly within the fractional model [2, 3, 23–34]. The FPT is defined as the time that the random walker takes to reach a target located in x_M for the first time, from a starting point x_0 . The FPT has been used to describe real physical processes such as animals searching for food [35], the passage of DNA molecules through a membrane channel [24] and the spreading of disease [36] etc. Moreover, the FPT distribution can be used to calculate other characteristic functions which are measured experimentally, such as the time evolution of an amount of a substance leaving a sample or the substance flux flowing through a sample surface.

In this paper we study subdiffusive systems. The FPT for subdiffusion was analyzed within the fractional model [23, 24] and [25] (the last one with a comment by Yuste and Lindenberg [26]), in the lattice and fractal medium [37, 38] and in the system with a subdiffusive membrane [34]. We derive the FPT distributions for subdiffusion equations derived from Sharma-Mittal, Tsallis and Gauss nonextensive entropies and compare them with the result obtained from the fractional model. Our strategy is as follows: we adapt Green's functions presented in their generalized forms as Frank's book [5] into special forms so that each of them exactly satisfies the relation (1). Next, we calculate the FPT distribution functions and compare them with the ones obtained from the fractional model. We derive consistency conditions in the functions calculated from various models in the long time limit. We briefly discuss the similarity of Green's functions and the interpretation of the parameters occurring in the nonextensive entropies and their connection with the parameters D_α and α , which are measured experimentally. This method would allow us to measure nonextensive entropy parameters.

II. THE METHOD

Here we will present the functions and equations which define Green's function and distribution of first passage time used in our considerations. The description of nonextensive entropies generating anomalous diffusion equations and their Green's functions, based on Frank's book [5], is presented in the Appendix.

A. Green's function

Green's function (GF) is defined as a solution to the appropriate diffusion equation with the initial condition

$$G(x, 0; x_0) = \delta(x - x_0) ,$$

δ denotes the delta-Dirac function. When the particles are independently transported and all of them are located at x_0 at the initial moment $t = 0$, Green's function can be interpreted as a concentration profile of the particles normalized to one (i.e. divided by the number of particles). The stochastic interpretation of the GF is that it is treated as a probability density of finding a particle at point x in time t under the condition that the initial position of the one is x_0 . For the unrestricted system the GF satisfies the natural boundary conditions which require the disappearance of the function at an infinite distance from the initial position $G(x, t; x_0) \rightarrow 0$, when $x \rightarrow \pm\infty$. In our paper we use Green's function for the system with a fully absorbing wall. The commonly used boundary condition at an absorbing wall reads

$$G_{\text{abs}}(x_M, t; x_0) = 0 .$$

The GF for the normal and subdiffusive systems with a fully absorbing wall can be found through the means of the method of images, which for $x, x_0 < x_M$ gives

$$G_{\text{abs}}(x, t; x_0) = G(x, t; x_0) - G(x, t; 2x_M - x_0) . \quad (2)$$

B. First passage time

Let us assume that a particle is located at x_0 at the initial moment $t = 0$. The time when the particle reaches the point x_M for the first time is a random variable described by a probability density of F , calculated according to the formula for $t > 0$

$$F(t; x_0, x_M) = -\frac{dP(t; x_0, x_M)}{dt} , \quad (3)$$

for $t \leq 0$ we put $F(t; x_0, x_M) = 0$, and where $P(t; x_0, x_M)$ denotes the probability of finding the particle at time t starting from x_0 in the system with a fully absorbing wall located at x_M (in the following we assume that $x_0 < x_M$)

$$P(t; x_0, x_M) = \int_{-\infty}^{x_M} G_{\text{abs}}(x, t; x_0) dx . \quad (4)$$

The cumulative function $R(t; x_0, x_M) = \int_{-\infty}^t F(t; x_0, x_M) dt$ reads

$$R(t; x_0, x_M) = 1 - P(t; x_0, x_M) .$$

The mean first time $\langle T \rangle$ is defined as

$$\langle T \rangle = \int_0^{\infty} t F(t; x_0, x_M) dt .$$

Assuming that $tP(t; x_0, x_M) \rightarrow 0$ when $t \rightarrow \infty$, one obtains

$$\langle T \rangle = \int_0^{\infty} P(t; x_0, x_M) dt . \quad (5)$$

III. GREEN'S FUNCTIONS AND FIRST PASSAGE TIME DISTRIBUTIONS

Green's functions (A.3), (A.4) and (A.5), presented in the Appendix, depend on the parameters of q which can be interpreted as a measure of nonextensivity entropy and the fluctuation strength Q_i , here the index i denotes the model, $i = SM, T, G$ for the Sharma–Mittal, Tsallis and Gauss models respectively. Sharma–Mittal Green's function additionally depends on the parameter r . Green's function for the Tsallis and Gauss models can be treated as specific cases of Sharma–Mittal Green's function, using $q = r$ for the Tsallis model and having as a limit $r \rightarrow 1^-$ for Gauss model. However, retaining the commonly used terminology, we consider these functions separately.

We look at two sets of subdiffusive models having different physical origins. The first contains the models derived from nonextensive entropy and the second, contains the fractional model. In general, both of these sets can describe the same physical processes. However, there also occur processes which can be described by models from one set alone, the other set of models cannot be applicable to describe this process (this problem will be briefly discussed in the Final Remarks). We are going to find the accordance conditions between models from both sets using the FPT distributions. Our further considerations are based on the following assumptions: the first, since all models describe the same subdiffusion process, all of Green's functions should provide the same relation which defines subdiffusion (1); the second, all Greens functions depend on two parameters α and D_α ; the third, the parameters α and D_α are measured experimentally within the fractional model. Our last assumption is supported by the fact that the subdiffusion parameters D_α and α are measured experimentally [39–41] by means of, for example, the time evolution of the near membrane layer. The fluctuation strength Q_i , which in general depends on q and r , plays the key role in expressing the parameters of the models based on nonextensive entropy by α and D_α . When $q = r = 1$ we are dealing with normal diffusion and then Q_i is identified as the twofold normal diffusion coefficient, $D_1 = 2Q_i$ for each model. Taking into account Eqs. (1), (A.6), (A.7), (A.8), (A.11), and (A.12) we come to the conclusion that relation (1) will be satisfied by all of Green's functions $G_i(x, t; x_0)$ when

$$q = \frac{2}{\alpha} - 1 \quad (6)$$

for all models, while the fluctuation strength must be chosen for each model separately and taking into account (6) they read

$$Q_{SM} = \frac{\alpha [D_\alpha(3r-1)]^{1/\alpha}}{4r K_{r, 2/\alpha-1} |z_r|^{2(1-1/\alpha)}}, \quad (7)$$

$$Q_T = \frac{\alpha^2 [D_\alpha(6/\alpha-4)]^{1/\alpha}}{4(2-\alpha) |z_{2/\alpha-1}|^{2(1-1/\alpha)}}, \quad (8)$$

$$Q_G = \frac{\alpha D_\alpha^{1/\alpha}}{2 (\sqrt{2\pi e})^{2(1-1/\alpha)}}, \quad (9)$$

the coefficients z_r and $K_{r,q}$ are defined by Eqs. (A.9) and (A.10) in the Appendix, respectively. In the following subsections, we apply Eqs. (6) – (9) to eliminate the parameters q and Q_i from Green's functions (A.3), (A.4) and (A.5) and then we use modified Green's functions to calculate the functions $F_i(t; x_0, x_M)$ and $P_i(t; x_0, x_M)$ from (3) and (4). In the last subsection we will find these functions for the fractional model.

A. The Sharma–Mittal model

Using Eqs. (6), (7) and (A.3), Green's function for the homogeneous unrestricted system, provided by the Sharma–Mittal entropy model, reads

$$G_{SM}(x, t; x_0) = \frac{1}{\sqrt{D_\alpha(3r-1)t^\alpha |z_r|}} \left[\left\{ 1 - \frac{(r-1)(x-x_0)^2}{D_\alpha(3r-1)t^\alpha} \right\}_+ \right]^{\frac{1}{r-1}}, \quad (10)$$

where $r > 1/3$ and $r \neq 1$, $\{u\}_+ = \max\{u, 0\}$. The function has different properties depending on the value of the parameter r . In the following, we consider the cases $r > 1$ and $1/3 < r < 1$ separately.

1. The case of $r > 1$

The function (10) has a finite support for $r > 1$, so the probability of finding the particle differs from zero only in the interval

$$x \in (x_0 - W(t), x_0 + W(t)),$$

where $W(t) = Bt^{\alpha/2}$, $B = \sqrt{\frac{D_\alpha(3r-1)}{r-1}}$ (see Fig. 1). The boundaries of the interval move with the speed v_g given by the relation

$$v_g = \frac{dW(t)}{dt} = \frac{\alpha B}{2t^{1-\alpha/2}}. \quad (11)$$

The finiteness of v_g ensures that there is a minimum time T_{x_2, x_1} of the passing of the particle from the point x_1 to x_2 , which is given by the relation

$$T_{x_2, x_1} = \left[\frac{(x_2 - x_1)^2}{B^2} \right]^{1/\alpha}. \quad (12)$$

Using (2), (4), (10) and (12), we obtain

$$\begin{aligned} P_{SM, r>1}(t; x_0, x_M) &= \\ &= \Theta(T_{x_M, x_0} - t) + \Theta(t - T_{x_M, x_0}) \frac{2}{|z_r| \sqrt{r-1}} \\ &\quad \times \left(\frac{T_{x_M, x_0}}{t} \right)^{\alpha/2} {}_2F_1 \left[\frac{1}{2}, \frac{-1}{r-1}; \frac{3}{2}; \left(\frac{T_{x_M, x_0}}{t} \right)^\alpha \right], \end{aligned} \quad (13)$$

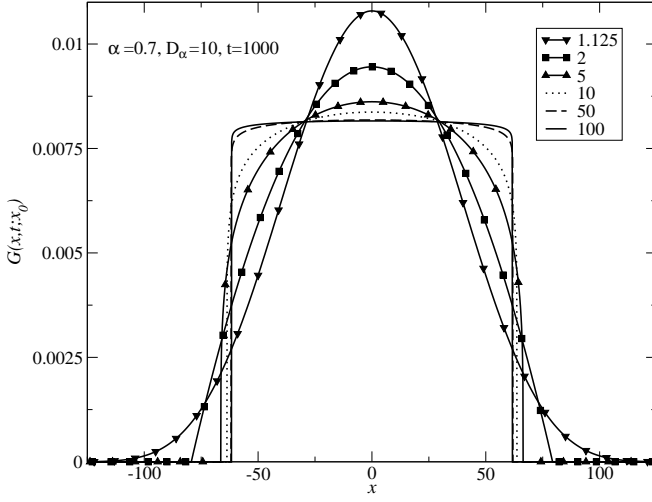


FIG. 1. Green's function for SM model in the case of $r > 1$ with finite support, $W = 154.7$ for $r = 1.125$, 79.3 for $r = 2$, 66.4 for $r = 5$, 63.7 for $r = 10$, 61.8 for $r = 50$ and 61.7 for $r = 100$, here $x_0 = 0$. Values of the parameter r are given in the legend.

where Θ is the Heviside function and ${}_2F_1[a, b; c; z]$ denotes the hypergeometric function,

$${}_2F_1[a, b; c; z] = \sum_{n=0}^{\infty} \frac{(a)_n (b)_n}{(c)_n} \frac{z^n}{n!}, \quad (14)$$

$(a)_n$ is the Pochhammer symbol, $(a)_n = \Gamma(a+n)/\Gamma(a)$. From (3) and (13) we obtain

$$\begin{aligned} F_{SM,r>1}(t; x_0, x_M) &= \\ &= \Theta(t - T_{x_M, x_0}) \frac{\alpha}{|z_r| \sqrt{r-1}} \\ &\times \frac{(T_{x_M, x_0})^{\alpha/2}}{t^{1+\alpha/2}} \left[1 - \left(\frac{T_{x_M, x_0}}{t} \right)^\alpha \right]^{\frac{1}{r-1}}. \end{aligned}$$

2. The case of $1/3 < r < 1$

For this case Green's function is unrestricted. The tails for a specific given t reads $G(x, t; x_0) \sim 1/x^{2/(1-r)}$ when $x \rightarrow \pm\infty$. The graphs of Green's functions for this case are presented in Fig. 2. By repeating the procedure presented above we obtain

$$\begin{aligned} P_{SM,r<1}(t; x_0, x_M) &= \\ &= \frac{2}{\sqrt{1-r}|z_r|} \left[\frac{(x_M - x_0)^2}{D_\alpha t^\alpha \left(\frac{3r-1}{1-r}\right) + (x_M - x_0)^2} \right] \\ &\times {}_2F_1 \left[\frac{1}{2}, \frac{1-3r}{2(1-r)}; \frac{3}{2}; \frac{(x_M - x_0)^2}{D_\alpha t^\alpha \left(\frac{3r-1}{1-r}\right) + (x_M - x_0)^2} \right], \end{aligned} \quad (15)$$

and

$$F_{SM,r<1}(t; x_0, x_M) =$$

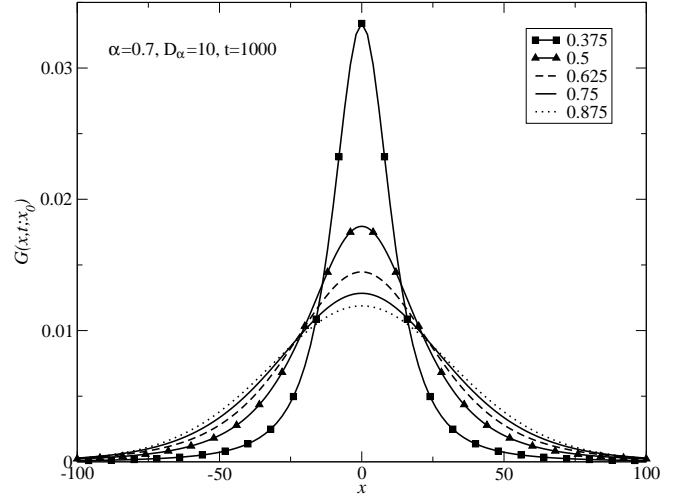


FIG. 2. Green's function G_{SM} for $1/3 < r < 1$. Values of the parameter r are given in the legend.

$$= \frac{\alpha |x_M - x_0|}{|z_r| \sqrt{1-r}} \frac{\left[D_\alpha \left(\frac{3r-1}{1-r} \right) \right]^{\frac{1+r}{2(1-r)}} t^{\frac{\alpha(1+r)}{2(1-r)} - 1}}{\left[D_\alpha \left(\frac{3r-1}{1-r} \right) t^\alpha + (x_M - x_0)^2 \right]^{\frac{1}{1-r}}}.$$

Eqs. (13), (14) and (15) provide the same formula for long times, namely for $t \gg t_{SM}$, where $t_{SM} = \left[\frac{(x_M - x_0)^2}{D_\alpha (3r-1)/(1-r)} \right]^{1/\alpha}$, we obtain

$$P_{SM}(t; x_0, x_M) = \frac{2|x_M - x_0|}{\sqrt{D_\alpha(3r-1)}|z_r|} \frac{1}{t^{\alpha/2}}, \quad (16)$$

for $r > 1/3$ and $r \neq 1$.

B. The Tsallis model

As we mentioned previously, Tsallis Green's function can be treated as the specific case of the Sharma–Mittal one. The results presented in the previous section are valid for the Tsallis model in which

$$r = \frac{2}{\alpha} - 1. \quad (17)$$

Let us note that the Tsallis model corresponds to the case of $r > 1$ for subdiffusion. As a formality we present the functions derived in Sec. III A 1 taking into account Eq. (17):

$$\begin{aligned} G_T(x, t; x_0) &= \\ &= \frac{\alpha}{2\sqrt{D_\alpha}(3-2\alpha)|z_{2/\alpha-1}|t^{\alpha/2}} \\ &\times \left[\left[1 - \frac{(1-\alpha)(x-x_0)^2}{(3-2\alpha)D_\alpha t^\alpha} \right] \right]_{+}^{\frac{\alpha}{2(\alpha-1)}}, \end{aligned} \quad (18)$$

where

$$z_{2/\alpha-1} = \alpha \frac{\Gamma\left(\frac{\alpha}{2(1-\alpha)}\right)}{\Gamma\left(\frac{1}{2(1-\alpha)}\right)} \sqrt{\frac{\pi}{2}} \frac{\alpha}{1-\alpha},$$

$$\begin{aligned} P_T(t; x_0, x_M) &= \\ &= \Theta(\tilde{T}_{x_M, x_0} - t) + \Theta(t - \tilde{T}_{x_M, x_0}) \frac{2\Gamma\left(\frac{1}{2(1-\alpha)}\right)}{\alpha\sqrt{\pi}\Gamma\left(\frac{\alpha}{2(1-\alpha)}\right)} \\ &\quad \times \left(\frac{\tilde{T}_{x_M, x_0}}{t}\right)^{\alpha/2} {}_2F_1\left[\frac{1}{2}, \frac{-\alpha}{2(1-\alpha)}; \frac{3}{2}; \left(\frac{\tilde{T}_{x_M, x_0}}{t}\right)^\alpha\right], \end{aligned} \quad (19)$$

where

$$\tilde{T}_{x_M, x_0} = \left[\frac{(2-\alpha)(x_M - x_0)^2}{2D_\alpha(3-2\alpha)}\right]^{1/\alpha},$$

and the distribution of the FPT is

$$\begin{aligned} F_T(t; x_0, x_M) &= \\ &= \Theta(t - \tilde{T}_{x_M, x_0}) \frac{\Gamma\left(\frac{1}{2(1-\alpha)}\right)}{\sqrt{\pi}\Gamma\left(\frac{\alpha}{2(1-\alpha)}\right)} \\ &\quad \times \frac{(\tilde{T}_{x_M, x_0})^{\alpha/2}}{t^{1+\alpha/2}} \left[1 - \left(\frac{\tilde{T}_{x_M, x_0}}{t}\right)^\alpha\right]^{\frac{1}{\alpha-1}}. \end{aligned}$$

For long times $t \gg t_T$, where $t_T = \left[\frac{(2-\alpha)(x_M - x_0)^2}{2D_\alpha(3-2\alpha)}\right]^{1/\alpha}$, Eq. (19) can be approximated as follows

$$P_T(t; x_0, x_M) = \frac{2|x_M - x_0|\sqrt{2(1-\alpha)}\Gamma\left(\frac{1}{2(1-\alpha)}\right)}{\alpha\sqrt{\alpha\pi}D_\alpha(6/\alpha - 4)\Gamma\left(\frac{\alpha}{2(1-\alpha)}\right)} \frac{1}{t^{\alpha/2}}.$$

C. The Gauss model

Green's function for the Gauss entropy model can be obtained from (10) in the limit $r \rightarrow 1^-$ and reads

$$G_G(x, t; x_0) = \frac{1}{\sqrt{2\pi D_\alpha t^\alpha}} \exp\left(-\frac{(x - x_0)^2}{2D_\alpha t^\alpha}\right). \quad (20)$$

From (4) and (20) we obtain

$$P_G(t; x_0, x_M) = \operatorname{erf}\left(\frac{x_M - x_0}{\sqrt{2D_\alpha t^\alpha}}\right), \quad (21)$$

where $\operatorname{erf}(u)$ is the error function

$$\operatorname{erf}(u) = \frac{2}{\sqrt{\pi}} \int_0^u e^{-u^2} du = \frac{2}{\sqrt{\pi}} \sum_{n=0}^{\infty} \frac{(-1)^n u^{2n+1}}{(2n+1)n!}. \quad (22)$$

Using (3) and (21) we get

$$F_G(t; x_0, x_M) = \frac{x_M - x_0}{\sqrt{2\pi D_\alpha}} \frac{1}{t^{1+\alpha/2}} e^{-\frac{(x_M - x_0)^2}{2D_\alpha t^\alpha}}.$$

For $t \gg t_G$, where $t_G = \left[\frac{(x_M - x_0)^2}{2D_\alpha}\right]^{1/\alpha}$, from (21) and (22) we obtain

$$P_G(t; x_0, x_M) = \frac{2|x_M - x_0|}{\sqrt{2\pi D_\alpha}} \frac{1}{t^{\alpha/2}}.$$

D. The fractional model

Within the fractional model, subdiffusion is described by the equation with the fractional Riemann–Liouville time derivative [2–4]

$$\frac{\partial P(x, t)}{\partial t} = \tilde{D}_\alpha \frac{\partial^{1-\alpha}}{\partial t^{1-\alpha}} \frac{\partial^2 P(x, t)}{\partial x^2},$$

with

$$\tilde{D}_\alpha = \frac{\Gamma(1+\alpha)D_\alpha}{2}. \quad (23)$$

Green's function is (in the following, the index F corresponds to the fractional model)

$$G_F(x, t; x_0) = \frac{1}{2\sqrt{D_\alpha}} f_{\alpha/2-1, \alpha/2}\left(t; \frac{|x - x_0|}{\sqrt{D_\alpha}}\right), \quad (24)$$

where

$$f_{\nu, \beta}(t; a) = \frac{1}{t^{1+\nu}} \sum_{k=0}^{\infty} \frac{1}{\Gamma(-k\beta - \nu)k!} \left(-\frac{a}{t^\beta}\right)^k, \quad (25)$$

$\beta, a > 0$, the function f can also be expressed in terms of the Fox function [42].

Applying Eqs. (2), (4) and (24) we get

$$P_F(t; x_0, x_M) = 1 - f_{-1, \alpha/2}\left(t; \frac{x_M - x_0}{\sqrt{D_\alpha}}\right), \quad (26)$$

and from (3) and (26) we obtain

$$F_F(t; x_0, x_M) = f_{0, \alpha/2}\left(t; \frac{x_M - x_0}{\sqrt{D_\alpha}}\right). \quad (27)$$

For $t \gg t_F$, where $t_F = \left[\frac{|x_M - x_0|\Gamma(1-\alpha/2)}{\sqrt{2D_\alpha}\Gamma(1-\alpha)}\right]^{2/\alpha}$, Eqs. (23), (25) and (26) give

$$P_F(t; x_0, x_M) = \frac{\sqrt{2}|x_M - x_0|}{\sqrt{D_\alpha}\Gamma(1+\alpha)\Gamma(1-\alpha/2)} \frac{1}{t^{\alpha/2}}. \quad (28)$$

We should add here, that the equivalent results to Eqs. (26), (27) and (28) were previously obtained by Barkai [23].

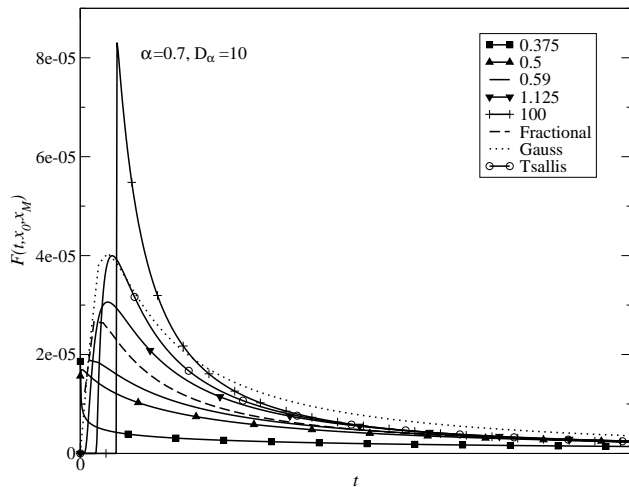


FIG. 3. Comparison between $F(t; x_0, x_M)$ for the Sharma–Mittal model for different r values and the other models.

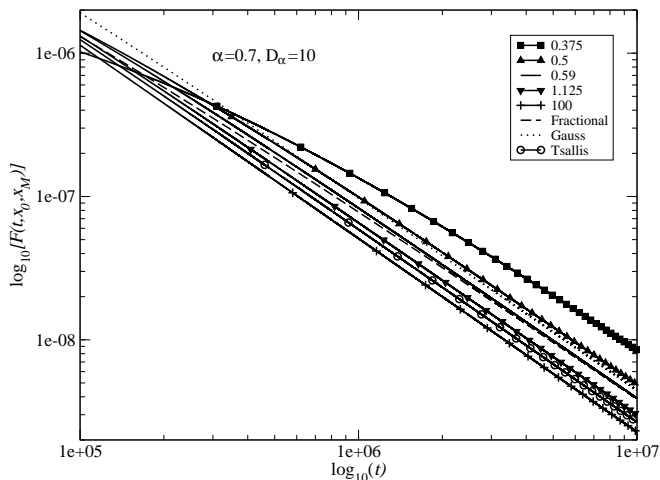


FIG. 4. The same situation as in Fig. 3 but in the log-log scale for long times.

IV. COMPARISON OF THE MODELS

In this section we compare the functions obtained from the different models. Putting the functions (13), (15), (19), (21), (26) into (5) respectively, we get $\langle T \rangle = \infty$ for all models.

The probability densities of FPT are presented in Figs. 3 and 4. In both graphs the functions obtained for the fractional model are represented by a dashed line, for the Tsallis model - by a solid one with empty circles and for the Gauss model - by a dotted line; the other lines are assigned to Sharma-Mittal functions with various r values. All graphs are prepared for $x_0 = 0$ and $x_M = 100$ and the values of the rest of the parameters are given in each figure separately (all quantities are given in the arbitrary chosen units). In Fig. 3 we have presented graphs for relatively short times calculated for all models studied in this paper, and in Fig. 4 we have presented

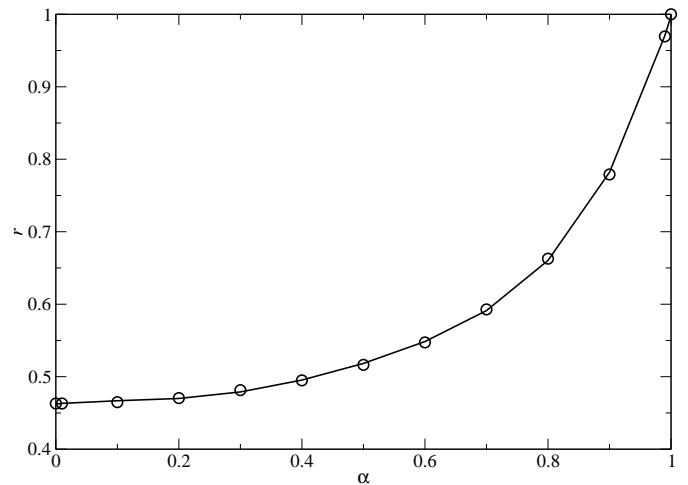


FIG. 5. Comparison of the numerical solutions of Eq. (30) (squares) and the plot of the function (31) (solid lines).

these functions for long times (in the log-log scale). We can observe that for a very short t the function F_{SM} is larger for a smaller r value (for $r > 1$ this function equals zero for $t < T_{x_M, x_0}$). For intermediate length times we observe the opposite situation, but the Gauss function is the largest now. For very long times, the situation again changes to the opposite and the largest value takes the function for the smallest r value, whereas the Gauss function takes medial values. In the log-log scale (Fig. 4) we observe that for sufficiently long times, the tails of $F(t; x_0, x_M)$ for all models and different r values are parallel, which shows that $F \sim 1/t^{1+\alpha/2}$ for long times. Let us note that the functions become parallel for a different time, and this time depends on the values of the ‘reference time’ t_i , $i = SM, G, T, F$. The t_{SM} heavily depends on the parameter r and for the cases presented in the graphs there are $t_{SM} = 192417$ for $r = 0.375$, 19307 for $r = 0.5$, 7650 for $r = 0.59$, 288 for $r = 1.125$ and 3981 for $r = 100$, the other reference times are: $t_T = 1767$, $t_G = 7173$, and $t_F = 794$. We would like to add that the graphs of the functions F_{SM} for various $1.125 < r < 100$ are located between the functions corresponding to $r = 1.125$ and $r = 100$ (for graphic clarity these functions are not presented in graphic figures), for $r > 100$ all functions are very similar, and in practice they are difficult to distinguish. Let us note that some of the functions F calculated from the Sharma–Mittal model are very similar to the ones obtained from fractional equations for sufficiently long times for some r parameters. We are going to find the conditions which ensure that the probability densities of FPT and their cumulative functions will be the same in the long time limit. For $t \gg \max\{t_{SM}, t_F\}$ the agreement condition reads

$$P_{SM}(t; x_0, x_M) = P_F(t; x_0, x_M), \quad (29)$$

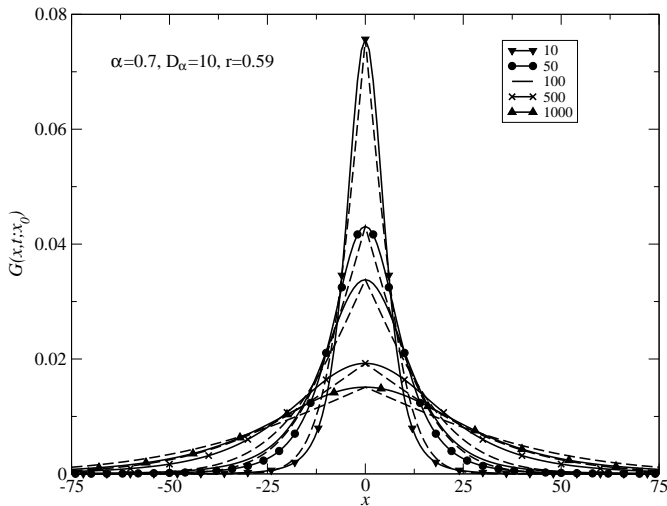


FIG. 6. Comparison between Green's function for the Sharma-Mittal (solid lines) and the fractional (dashed lines) models for different times given in the legend.

which is equivalent to

$$F_{SM}(t; x_0, x_M) = F_F(t; x_0, x_M).$$

From (16), (28) and (29) we get

$$\frac{1}{\Gamma(1-\alpha/2)} \frac{1}{\sqrt{\Gamma(1+\alpha)}} = \frac{\sqrt{2}}{\sqrt{3r-1}|z_r|}. \quad (30)$$

The numerical solution to Eq. (30) has a good approximation in the following form (see Fig. 5)

$$r = 3.008\alpha^5 - 5.471\alpha^4 + 3.768\alpha^3 - 0.869\alpha^2 + 0.101\alpha + 0.463. \quad (31)$$

We should note that function (31) gives $r \rightarrow 1$ when $\alpha \rightarrow 1^-$; this result to be expected since for $r = \alpha = 1$ all models provide Green's function for normal diffusion. The functions $G_{SM}(x, t; x_0)$ and $G_F(x, t; x_0)$ are also similar to each other for r given by Eq. (31), which is shown in Figs. 6 and 7. In Fig. 6 Green's functions for the Sharma-Mittal and the fractional models calculated for $\alpha = 0.7$ and various times are presented, in Fig. 7 for different α and t . Obviously, this similarity and the fact that the functions provide the relations (1) and (29) does not necessarily imply any equivalence between Green's functions, e.g. for fixed t and for $x \rightarrow \pm\infty$ $G_{SM}(x, t; x_0) \rightarrow (1/|x|)^{2/(1-r)}$, and while the asymptotic form $G_F(x, t; x_0) \sim |x| \exp(-a|x|^{1/(1-\alpha/2)})$ (a is a positive constant) has an exponential character and depends on α [2]. In Fig. 8 we can observe that the Green's function of the Sharma-Mittal and the fractional models are similar for r , which are calculated from (31), in contrast to the Gauss and Tsallis models, which do not fit each other. This is rather obvious since the subdiffusive Tsallis model corresponds to $r > 1$, whereas the Gauss one only is applicable for $r \rightarrow 1^-$.

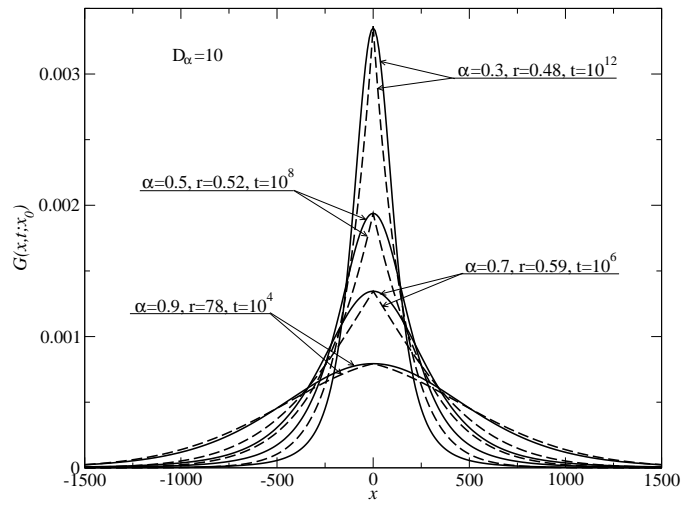


FIG. 7. Comparison between Green's function for different α and times given in the legend; r is calculated from (31) for each α separately. The additional description is the same as in Fig. 6.

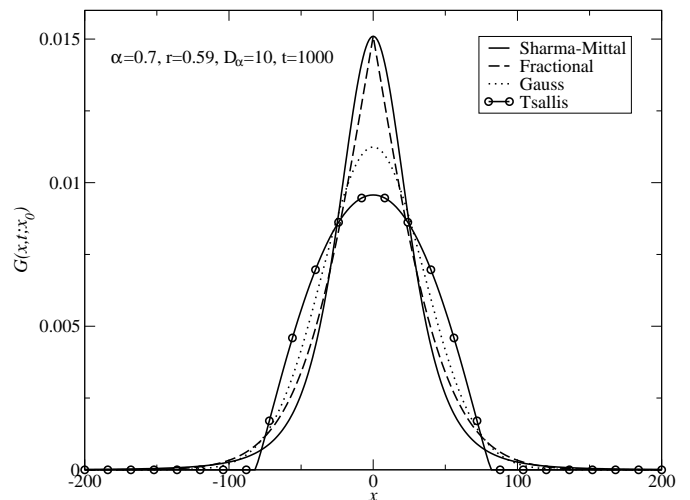


FIG. 8. Comparison between the Green's functions obtained from different models.

V. FINAL REMARKS

In this paper we have studied the subdiffusive first passage time distribution obtained from the Sharma-Mittal, Tsallis, Gauss and fractional models. The FPT probability densities were calculated from Green's functions which were chosen in such forms which exactly live up to relation (1). We have shown that the FPT probability distribution function and the function P calculated within the Sharma-Mittal model for r given by the formula (31), coincide with the ones obtained from the fractional model; P is a probability that a particle has not reached the arbitrary chosen point x_M until time t . This coincidence is independent of the subdiffusion coefficient D_α . The functions obtained from the Sharma-Mittal

model for $r > 1$ (which includes the Tsallis model) and for the nonextensive Gauss entropy model (which corresponds to the limit $r \rightarrow 1^-$ of Sharma-Mittal functions) do not coincide with the results of the fractional model. When r is not given by the formula (31), Eqs. (6), (7), (8) and (9) are still valid, but here α and D_α cannot be treated as parameters determined by the fractional model. In such a case, there are situations where the fractional model cannot be used but the other different models based on nonextensive entropy are applicable. Particular, for $r > 1$, the support of Green's function (10) is finite. In consequence, the subdiffusion process is achieved if the velocity of the borders decreases over time according to formula (11). Let us note that there are two mechanisms of the subdiffusion process. The first one depends on the motion of the borders which limit the area penetrated by the walker, the second is the process of the walker's movement within the allowed region. Since Green's functions with finite support and nonzero variance cannot describe an infinitely divisible process [43], the second mechanism cannot be considered as a random walk process in contrast with the fractional model.

A potential application of the Sharma-Mittal model for $r > 1$, is an animal searching for food. A similar problem was considered in [35], where the diffusion searching process was assumed to be at two stages. The first stage consists of searching for a diffusive type near the point where the animal stopped its 'quick movement' in order to find food, the second stage is the relatively fast movement made by the animal in order to change its searching region. This movement is assumed to be ballistic, e.g. with constant motion. Changing these assumptions, we get the model which — at least in our opinion — can be described by Sharma-Mittal Green's function. Namely, we assume that the animal movement in the restricted region (stage 2) is carried out with velocity decreasing over time according to formula (11). The diminishing velocity is connected with the animal energy, which is gradually lost, especially in the system of a complex structure. In stage 1, searching inside the restricted region can be governed by some specific mechanisms, which are not, in fact, random walk, and which provide a finite space domain.

Now we shall turn our attention to discussing a method of extracting the subdiffusion parameters occurring in a nonextensive entropy model from experimental data (a similar problem was considered in [44]). The parameters q and Q_i can be calculated from Eqs. (6), (7), (8) and (9). The parameters α and D_α are defined by Eq. (1), but this equation does not lend itself to experimental assignment. Therefore, one needs to use other functions, which can be measured experimentally. One of such functions is the amount of substances $M(t; x_M)$ leaving a semi-infinite medium occupying the region $(-\infty, x_M)$ as a function of time (then the surface located at x_M can be treated as a fully absorbing membrane) or the flux $J(t; x_M)$ flowing through the surface. It is easy to see that the func-

tions M and J depend on the FPT characteristics as follows $M(t; x_M) = \int_{-\infty}^{x_M} C(x_0, 0)[1 - P_i(x_M, t; x_0)]dx_0$ and $J(t; x_M) = \int_{-\infty}^{x_M} C(x_0, 0)F_i(x_M, t; x_0)dx_0$, where $i = SM, T, G, F$ and $C(x_0, 0)$ is the initial concentration. When r is given by (31), we get $M_{SM}(t; x_M) = M_F(t; x_M)$ and $J_{SM}(t; x_M) = J_F(t; x_M)$ in the long time limit. Thus, assuming that $r > 1$, each measurement of M and J gives the parameter values which can be taken from the fractional model.

Here we shall focus on the method of extracting the parameters from experimental data using the fractional model. Since Eq. (31) ensures the coincidence of first passage time distribution for the Sharma-Mittal and fractional models for long times, the comparison FPT functions with experimental data provide the same parameter values α and D_α as for the fractional model. Since the fractional model gives the parameters using a different method, for example, time evolution of a near-membrane layer [39, 40] or the reaction front in a system with chemical reactions [45], we can use the subdiffusion parameters obtained through the means of any method within the fractional model. To illustrate this we will calculate now the parameters for the subdiffusion of glucose and sucrose in gel (1.5 per cent water solution of agarose). The subdiffusion parameters found in [39, 40] are: $\alpha = 0.90 \pm 0.01$, $\tilde{D}_{0.90} = (9.8 \pm 1.0) \times 10^{-4} mm^2/s^{0.90}$ for glucose, and $\tilde{D}_{0.90} = (6.3 \pm 0.9) \times 10^{-4} mm^2/s^{0.90}$ for sucrose. Taking r calculated from (31) and using Eqs. (6), (7) and (23) we get $q = 1.22$ and $Q_{SM} = 6.43 \times 10^{-4} mm^{2.22}/s$ for glucose, $Q_{SM} = 3.93 \times 10^{-4} mm^{2.22}/s$ for sucrose (we have omitted here the error calculations).

To extract the subdiffusion parameters from experimental data for the Sharma-Mittal model when $r > 1$, it is possible to measure the velocity of the borders $v(t)$, which allows one to determine the parameters α and B . We remark that a similar approach was used to find the parameters of the cut-off distribution of postural sway; the estimation of the border locations allow us to calculate the distribution parameters [46]. However, in this case, the process was not considered as a stochastic one continuously changing over time, but only two arbitrary chosen 'times' (postural sway for the old and young) were taken into account. Since for $r \rightarrow \infty$ Green's function approaches a constant distribution [46], r can be interpreted as the 'measure' of the deviation of the probability density of constant distribution. Therefore, r represents the 'uncertainty' of finding the walker in the near-border regions.

Appendix: Anomalous diffusion equation derived from nonextensive entropy

The Sharma-Mittal entropy is defined as

$$S_{q,r}^{SM}[P] = \frac{1 - \left(\int_{\Omega} P^r dx\right)^{(q-1)/(r-1)}}{q-1}, \quad (\text{A.1})$$

where $q, r > 0$, $q, r \neq 1$, and the Gauss entropy reads

$$S_q^G[P] = \frac{1 - e^{(q-1) \int P \ln P dx}}{q-1},$$

where $q > 0$, $q \neq 1$, The Tsallis entropy can be obtained from (A.1) putting $q = r$.

The anomalous diffusion equation reads

$$\frac{\partial P(x, t)}{\partial t} = Q_i \Psi_i[P] \frac{\partial^2 P^r(x, t)}{\partial^2 x}, \quad (\text{A.2})$$

where $r = q (\neq 1, > 1/3)$ for the Tsallis case and $r = 1$ for the Gauss one, the index i denotes the symbol identifying entropy, $\{u\}_+ = \max\{u, 0\}$, Q_i denotes the fluctuation strength, and

$$\Psi_{SM}[P] = \left(\int P^r dx \right)^{\frac{q-r}{r-1}}, \quad \Psi_T[P] = 1,$$

$$\Psi_G[P] = e^{(q-1) \int P \ln P dx}.$$

Green's functions of (A.2) for different models are

$$\begin{aligned} G_{SM}(x, t; x_0) &= \\ &= D_{SM}(t) \left[\left\{ 1 - \frac{C_{SM}(t)}{2} (r-1)(x-x_0)^2 \right\}_+ \right]^{\frac{1}{r-1}}, \end{aligned} \quad (\text{A.3})$$

where $r > 1/3$, $r, q \neq 1$, $q > 0$,

$$\begin{aligned} G_T(x, t; x_0) &= \\ &= D_T(t) \left[\left\{ 1 - \frac{C_T(t)}{2} (q-1)(x-x_0)^2 \right\}_+ \right]^{\frac{1}{q-1}}, \end{aligned} \quad (\text{A.4})$$

where $q > 1/3$, $q \neq 1$,

$$G_G(x, t; x_0) = D_G(t) \exp \left(-\frac{C_G(t)}{2} (x-x_0)^2 \right). \quad (\text{A.5})$$

The functions occurring in (A.3)–(A.5) are defined as

$$D_{SM}(t) = \left[\frac{1}{2r(1+q)Q_{SM}K_{r,q}|z_r|^2 t} \right]^{\frac{1}{1+q}}, \quad (\text{A.6})$$

$$D_T(t) = \left[\frac{1}{2q(1+q)Q_T|z_q|^2 t} \right]^{\frac{1}{1+q}}, \quad (\text{A.7})$$

$$D_G(t) = \left[\frac{\sqrt{e}^{q-1}}{2\pi(1+q)Q_G t} \right]^{\frac{1}{1+q}}, \quad (\text{A.8})$$

where

$$z_r = \begin{cases} \sqrt{\frac{\pi}{r-1} \frac{\Gamma(r/(r-1))}{\Gamma((3r-1)/(2(r-1)))}}, & r > 1, \\ \sqrt{\pi}, & r = 1, \\ \sqrt{\frac{\pi}{1-r} \frac{\Gamma((1+r)/2(1-r))}{\Gamma(1/(1-r))}}, & 1/3 < r < 1. \end{cases} \quad (\text{A.9})$$

and

$$K_{r,q} = \begin{cases} \left(\frac{3r-1}{2r} \right)^{\frac{q-r}{r-1}}, & r \neq 1, \\ (\sqrt{e})^{1-q}, & r = 1, \end{cases} \quad (\text{A.10})$$

$$\begin{aligned} C_{SM}(t) &= 2(z_r D_{SM}(t))^2, \\ C_T(t) &= 2(z_q D_T(t))^2, \\ C_G(t) &= 2\pi(D_G(t))^2. \end{aligned} \quad (\text{A.11})$$

The second moment of Green's functions presented above can be calculated according to the formulae

$$\begin{aligned} \langle (\Delta x)^2(t) \rangle_{SM} &= \frac{2}{3r-1} \frac{1}{C_{SM}(t)}, \\ \langle (\Delta x)^2(t) \rangle_T &= \frac{2}{3q-1} \frac{1}{C_T(t)}, \\ \langle (\Delta x)^2(t) \rangle_G &= \frac{1}{C_G(t)}. \end{aligned} \quad (\text{A.12})$$

-
- [1] J. Bouchaud and A. Georges, Phys. Rep., **195**, 127 (1990).
[2] R. Metzler and J. Klafter, Phys. Rep., **339**, 1 (2000).
[3] R. Metzler and J. Klafter, J. Phys. A, **37**, R161 (2007).
[4] A. Compte, Phys. Rev. E, **53**, 4191 (1996).
[5] T. Frank, *Nonlinear Fokker-Planck Equations. Fundamental and Applications* (Springer, Berlin, 2005).
[6] C. Tsallis, *Introduction to Nonextensive Statistical Mechanics* (Springer, NY, 2009).
[7] A. Plastino and A. Plastino, Physica A, **222**, 347 (1995).
[8] L. Borland, F. Pennini, A. Plastino, and A. Plastino, Eur. Phys. J. B, **12**, 285 (1999).
[9] A. Compte and D. Jou, J. Phys. A: Math. Gen., **29**, 4321 (1996).
[10] C. Tsallis and D. Bukman, Phys. Rev. E, **54**, R2197 (1996).
[11] G. Drazer, H. Wio, and C. Tsallis, Granular Matter, **3**, 105 (2001).
[12] T. Frank, Physica A, **310**, 397 (2002).
[13] A. Scarfone and T. Wada, Braz. J. Phys., **39**, 475 (2009).
[14] T. Frank and A. Daffertshofer, Physica A, **285**, 351 (2000).
[15] K. Wang and M. Tokuyama, Physica A, **265**, 341 (1999).
[16] T. Frank, Physica A, **301**, 52 (2001).
[17] T. Frank, Physica A, **331**, 391 (2004).
[18] L. Borland, Phys. Rev. E, **57**, 6634 (1998).
[19] D. Stariolo, Phys. Lett. A, **185**, 262 (1994).
[20] E. Curado and F. Nobre, Phys. Rev. E, **67**, 021107

- (2003).
- [21] S. Render, *A Guide to First-Passage Processes* (Cambridge UP, Cambridge, 2001).
- [22] B. Hughes, *Random Walks and Random Environments, vol. I* (Oxford UP, New York, 1995).
- [23] E. Barkai, Phys. Rev. E, **63**, 046118 (2001).
- [24] R. Metzler and J. Klafter, Biophys. J, **85**, 2776 (2003).
- [25] M. Gitterman, Phys. Rev. E, **62**, 6065 (2000).
- [26] S. Yuste and K. Lindenberg, Phys. Rev. E, **69**, 033101 (2004).
- [27] E. Lenzi, C. Anteneodo, and L. Borland, Phys. Rev. E, **63**, 051109 (2001).
- [28] B. Dybiec, E. Gudowska-Nowak, and P. Hänggi, Phys. Rev. E, **73**, 046104 (2006).
- [29] A. Chechkin, R. Metzler, V. Gonchar, J. Klafter, and L. Tanatarov, J. Phys. A: Math. Gen., **36**, L537 (2003).
- [30] T. Koren, A. Chechkin, and J. Klafter, Physica A, **379**, 10 (2007).
- [31] A. Amitai, Y. Kantor, and M. Kardar, Phys. Rev. E, **81**, 011107 (2010).
- [32] E. Lenzi, L. Evangelista, M. Lenzi, and L. da Silva, Phys. Rev. E, **80**, 021131 (2009).
- [33] K. Fa and E. Lenzi, Phys. Rev. E, **71**, 012101 (2005).
- [34] T. Kosztolowicz and K. Lewandowska, Acta Phys. Pol. B, **40**, 1437 (2009).
- [35] O. Bénichou, M. Coppey, P. Suet, and R. Voituriez, Phys. Rev. Lett., **94**, 198101 (2005).
- [36] A. Lloyd and R. May, Science, **292**, 1316 (2001).
- [37] S. Condamin, V. Tejedor, O. Bénichou, and J. Klafter, PNAS, **105**, 5675 (2008).
- [38] S. Condamin, O. Bénichou, and J. Klafter, Phys. Rev. Lett., **98**, 250602 (2007).
- [39] T. Kosztolowicz, K. Dworecki, and S. Mrówczyński, Phys. Rev. E, **71**, 041105 (2005).
- [40] T. Kosztolowicz, K. Dworecki, and S. Mrówczyński, Phys. Rev. Lett., **94**, 170602 (2005).
- [41] A. Klemm, R. Metzler, and R. Kimmich, Phys. Rev. E, **65**, 021112 (2002).
- [42] T. Kosztolowicz, J. Phys. A, **37**, 10779 (2004).
- [43] W. Feller, *An Introduction to Probability Theory and Its Applications* (Wiley, New York, 1968).
- [44] T. Frank and R. Friedrich, Physica A, **347**, 65 (2005).
- [45] T. Kosztolowicz and K. Lewandowska, Phys. Rev. E, **78**, 066103 (2008).
- [46] T. Frank, Physica A, **388**, 2503 (2009).